

# Photoinduced Electron Transfer and Intramolecular Folding in a Tricarbonylrhenium (Bi)pyridine Based Donor/Crown/Acceptor Assembly: Dependence on Solvent

Christine A. Berg-Brennan, Dong I. Yoon, Robert V. Slone, Amy P. Kazala, and Joseph T. Hupp\*

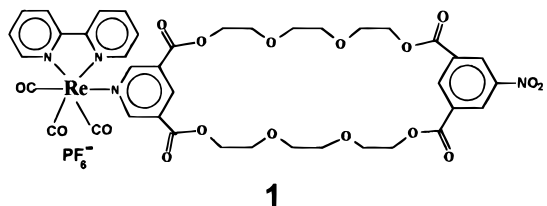
Department of Chemistry, Northwestern University, Evanston, Illinois 60208

Received May 3, 1995<sup>⊗</sup>

The title assembly displays an emissive rhenium-to-pyridine charge-transfer state that is partially quenched by electron transfer to an attached acceptor (nitrobenzene). Quenching is preceded by intramolecular folding (*J. Am. Chem. Soc.* **1993**, *115*, 2048). Variable-temperature quenching measurements can be used to determine the characteristic temperature,  $T_{tr}$ , above which unfolded photoexcited state conformations become favored over folded conformations. Similar information for the ground state can be obtained from variable-temperature NMR measurements. Studies in eight solvents show that excited state folding is (1) enthalpically favored but entropically disfavored (all solvents), (2) correlated (via  $T_{tr}$ ) with the inverse dielectric strength of the solvent, and (3) enhanced in comparison to folding in the electronic ground state (studies in one solvent). The combined evidence points to a folding reaction that is driven by optimization of localized Coulombic interactions. Optimization of solvent cohesive interactions, however, may possibly also play a role in the folding reaction.

## Introduction

Recently we reported on the synthesis and photoredox reactivity of crown-ether-linked assemblies featuring tricarbonylrhenium (bi)pyridine species as donors and nitrobenzene as an acceptor.<sup>1,2</sup> For assembly **1**, the redox sequence involves

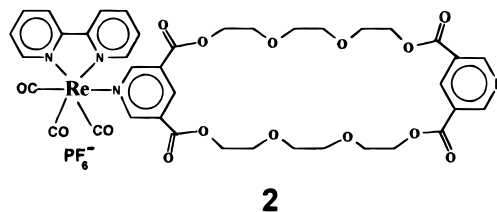


rhenium-to-pyridine charge-transfer absorption, followed by pyridine anion reduction of nitrobenzene (NB) and eventually electron transfer (ET) from nitrobenzene anion back to Re(II). The ultimate goal with the assemblies is to understand how noncovalently bound material (i.e., crown-encapsulated material) can modulate or facilitate intermediate to long-range ET kinetics. Preliminary studies with an *empty* crown assembly (**1**) revealed that the rate of light-induced forward ET ( $py^- \rightarrow NB$ ) is strongly dependent on the initial assembly conformation and that the conformation, in turn, is strongly dependent on temperature.<sup>2</sup> Thus, at low temperatures, ET occurs directly from a folded conformation, while at high temperatures it occurs only after uphill folding from an initially open form. We now report that the unusual folding phenomenon and, therefore, the kinetics display a significant dependence on solvent. We additionally report that the folding energetics depend significantly on the internal oxidation state distribution. Together the two effects provide useful insights into the chemical origins of the phenomenon.

## Experimental Section

**Materials.** Assembly **1** was prepared as previously described.<sup>1</sup> Complex **2** was prepared and purified similarly except that a macro-

cyclic ligand containing a second pyridine was used in place of the



nitrobenzene-containing ligand. (Analytical, FAB mass spectral, and <sup>1</sup>H NMR data for **2** have been reported as Supplemental Material in ref 1.) The required dipyriddy macrocycle was prepared via the method outlined previously for the nitrobenzene-containing ligand<sup>1</sup> except that dicesium 3,5-pyridinedicarboxylate was used in place of dicesium 5-nitroisophthalate for macrocycle closure.

Propionitrile (99%), 2-butanone (99.5%), methyl benzoate (99%), and 1,3-dichloropropane (99%) were used as received from Aldrich Chemical Co. HPLC grade acetone and chloroform were used as received from Fisher. Dichloromethane (HPLC grade, Fisher) was dried by distillation from calcium hydride. Nitroethane (99.5%, Aldrich) was decolorized and dried by passage through an activated alumina column.

**Measurements.** One-dimensional NOE measurements were made in CD<sub>2</sub>Cl<sub>2</sub> by using a 600 MHz Bruker spectrometer. Time-resolved luminescence measurements were made by exciting deoxygenated solutions of **1** or **2** (nitrogen atmosphere) with a PRA model LN102 dye laser (386 nm) that was pumped by a PRA Model LN1000 nitrogen laser (~5 Hz; 300–700 ps pulse width). Emitted light (570 nm) was collected at 90° and focused onto a Jarrell Ash monochromator that exited to a Hamamatsu R928 photomultiplier tube. In order to enhance the system response time, the R928 was configured to utilize only five dynodes. Tube saturation was avoided by employing neutral density filters. The output of the tube was collected and processed with either a LeCroy 6880 digitizer (400 MHz bandwidth) or a LeCroy 9400 digital oscilloscope (125 MHz bandwidth). Processing consisted of digitizing and averaging 50–200 shots per run. Several runs were then combined and further averaged. The averaged signals were then fit to a single-exponential decay function where the first 6 ns of data were discarded because of slow instrument response. Sample temperatures were controlled with either an Oxford Instruments Model DN1704 liquid nitrogen cryostat (180–295 K) or a water bath connected to a home-built heat exchanger and a circulating reservoir (300–350 K). Sample concentrations typically were  $5 \times 10^{-6}$  M.

<sup>⊗</sup> Abstract published in *Advance ACS Abstracts*, February 15, 1996.

(1) Yoon, D. I.; Berg-Brennan, C. A.; Lu, H.; Hupp, J. T. *Inorg. Chem.* **1992**, *31*, 3192.

(2) Berg-Brennan, C. A.; Yoon, D. I.; Hupp, J. T. *J. Am. Chem. Soc.* **1993**, *115*, 2048.

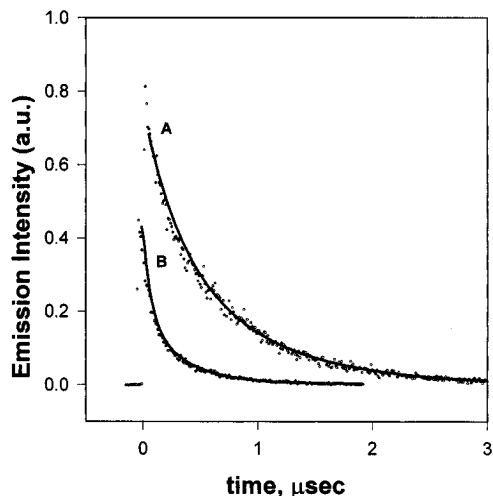


**Figure 1.** Charge-transfer excited state decay curves (luminescence) for **1** in deoxygenated chloroform as solvent. Lines shown are best fit lines to a single-exponential decay function. Curve A:  $T = 240$  K. Curve B:  $T = 343$  K.

**Table 1.** Luminescence Lifetimes and Intramolecular Quenching Rate Constants as a Function of Temperature in Deoxygenated Acetone as Solvent

$T, K$	$\tau_1, ns$	$\tau_2, ns$	$10^{-6}k_{obs}, s^{-1}$
290	$98 \pm 4$	$337 \pm 6$	7.6
280	$100 \pm 2$	$340 \pm 5$	7.1
270	$101 \pm 4$	$346 \pm 5$	7.0
260	$105 \pm 2$	$352 \pm 6$	6.7
250	$111 \pm 4$	$344 \pm 5$	6.1
240	$120 \pm 4$	$349 \pm 5$	5.5
230	$131 \pm 4$	$351 \pm 8$	4.8
220	$148 \pm 6$	$343 \pm 9$	3.8
210	$174 \pm 6$	$350 \pm 10$	2.9
200	$235 \pm 13$	$350 \pm 10$	1.4
190	$255 \pm 4$	$357 \pm 7$	1.1
183	$273 \pm 5$	$370 \pm 10$	0.96

Rate constants ( $k_{obs}$ ) for intramolecular quenching of the emissive excited state were obtained from differences in inverse lifetime ( $1/\tau$ ; eq 1) for complex **1** (appended quencher) versus **2** (no quencher).<sup>1,2</sup>

$$1/\tau_1 - 1/\tau_2 = k_{obs} \quad (1)$$

## Results and Discussion

Figure 1 shows representative emission decay curves for **1** at low and high temperatures in chloroform as solvent. Table 1 summarizes similar data for both **1** and **2** in acetone as solvent and also lists  $k_{obs}$  values derived from eq 2. Figure 2 shows a plot of the logarithm of the observed electron transfer rate constant versus the inverse temperature in a third solvent (nitroethane). From the figures and table, electron transfer quenching clearly is thermally activated. Figure 2 shows that two distinct activation regimes exist in acetone, with a transition temperature ( $T_{tr}$ ) of 225 K. (Similar behavior occurs in other solvents.) From the slope of the plot in the high-temperature regime,  $\Delta H_{obs}^\ddagger$  is 1.7 kcal mol<sup>-1</sup>.<sup>3</sup> The corresponding preexponential factor,  $A_{obs}$ , is  $8 \times 10^7$  s<sup>-1</sup>. In contrast, in the low-temperature regime,  $\Delta H_{obs}^\ddagger$  is 4.6 kcal mol<sup>-1</sup> and  $A_{obs}$  is  $5 \times 10^{10}$  s<sup>-1</sup>. We have previously shown (with CH<sub>2</sub>Cl<sub>2</sub> as solvent) that multicomponent activation behavior is consistent with

(3) The superscript dagger notation is typically used in the electron-transfer literature to designate activation parameters determined from plots of  $\ln(k_{obs}/T)$  versus  $1/T$  ("Eyring" plots), while asterisks are used for parameters derived from plots of  $\ln k_{obs}$  versus  $1/T$  (e.g., Figure 1). Nevertheless, the dagger notation is employed here for  $\ln k_{obs}$  vs.  $1/T$  parameters to avoid confusion with the asterisk notation for electronic excited states (cf. Scheme 1).

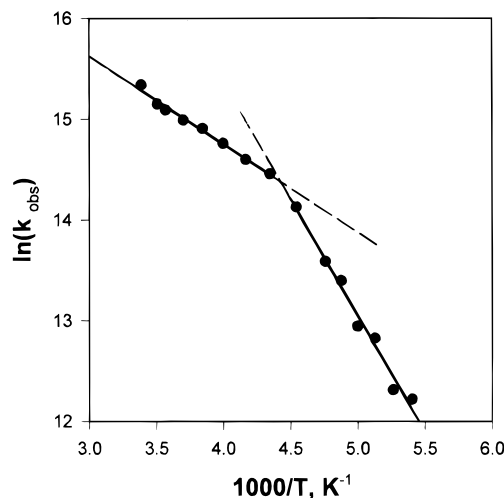
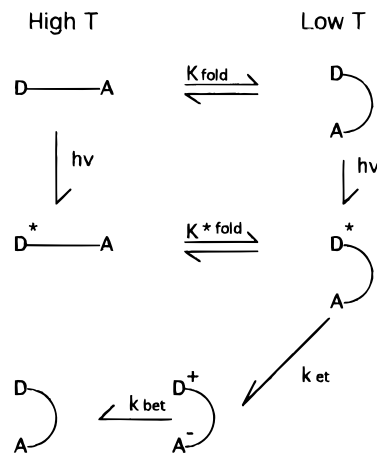


**Figure 2.** Logarithm of  $k_{obs}$  versus inverse temperature in deoxygenated nitroethane as solvent.

## Scheme 1



Scheme 1.<sup>2</sup> From the scheme, the observed low-temperature rate and activation parameters can be identified directly with the parameters for the ET step ( $k_{obs}(\text{low } T) = k_{ET}$ ;  $\Delta H_{obs}^\ddagger(\text{low } T) = \Delta H_{ET}^\ddagger$ ;  $A_{obs}(\text{low } T) = A_{ET}$ ). At high temperatures, on the other hand, the observed parameters are interpreted as sums (or products) of preequilibrium folding parameters and ET activation or rate parameters, i.e.<sup>2</sup>

$$k_{obs}(\text{high } T) = K_{folding}^* k_{ET} \quad (2)$$

$$\Delta H_{obs}^\ddagger(\text{high } T) = \Delta H_{folding}^\circ + \Delta H_{ET}^\ddagger \quad (3)$$

$$R \ln A_{obs}(\text{high } T) = \Delta S_{folding}^\circ + R \ln A_{ET} \quad (4)$$

From the data in Figure 2,  $\Delta H_{folding}^\circ$  is  $-2.9$  kcal mol<sup>-1</sup> and  $\Delta S_{folding}^\circ$  is  $-13$  eu. The combined parameters define a temperature ( $T_{tr}$ ) above which folding in the photoexcited state is thermodynamically disfavored (i.e.,  $K_{folding}^* < 1$ ). Nevertheless, from Scheme 1 the actual ET step, at all temperatures, takes place from a folded conformation.

The variable-temperature rate studies have been extended to a total of eight solvents. All eight yield multicomponent activation behavior,<sup>4</sup> with activation enthalpies and preexponential factors that are smaller in the high- $T$  regime than in the low- $T$  regime (see Table 2). It follows (eqs 3 and 4) that  $\Delta H_{folding}^\circ$  and  $\Delta S_{folding}^\circ$  must, in all cases, be negative. Observed transition temperatures range from 222 to nearly 300 K.

**Table 2.** Activation Parameters for Photoinduced Electron Transfer in (bpy)Re(CO)<sub>3</sub>(py-crown-NB)<sup>+</sup> in Various Solvents

solvent	$\Delta H^\ddagger(\text{high } T)$ , kJ/mol	$\Delta H^\ddagger(\text{low } T)$ , kJ/mol	$\Delta H^\ddagger_{\text{folding}}$ , kJ/mol	$T_{\text{tr}}$ , K	$A(\text{high } T)$ , s <sup>-1</sup>	$A(\text{low } T)$ , s <sup>-1</sup>	$\Delta S^\circ_{\text{folding}}$ , J/(mol·K)
acetone	3.6 ± 0.1	12.3 ± 0.2	-8.7 ± 0.3	235	3 × 10 <sup>7</sup>	3 × 10 <sup>9</sup>	-40
2-butanone	4.2 ± 0.2	8.2 ± 0.5	-4.0 ± 0.7	242	7 × 10 <sup>7</sup>	2 × 10 <sup>8</sup>	-10
chloroform	0.8 ± 0.7	14 ± 4	-13 ± 5	294	1.3 × 10 <sup>6</sup>	3 × 10 <sup>8</sup>	-50
dichloromethane	6.0 ± 0.3	37.4 ± 0.8	-31 ± 1	280	3 × 10 <sup>6</sup>	2 × 10 <sup>12</sup>	-110
1,3-dichloropropane	10 ± 8	19.4 ± 0.4	-9 ± 8	~280	2 × 10 <sup>7</sup>	4 × 10 <sup>9</sup>	-40
methyl benzoate	8 ± 20	34 ± 3	-26 ± 23	~290	7 × 10 <sup>7</sup>	2 × 10 <sup>12</sup>	-90
nitroethane	7.2 ± 0.2	19.2 ± 0.2	-12 ± 0.4	225	8 × 10 <sup>7</sup>	5 × 10 <sup>10</sup>	-50
propionitrile	5.5 ± 0.6	20.6 ± 0.4	-15 ± 1	222	5 × 10 <sup>7</sup>	2 × 10 <sup>11</sup>	-70

As perhaps suggested by the wide variations in transition temperature, both the activation parameters and the folding parameters are sensitive to the identity of the solvent. To understand the variations in the folding parameters, in particular, we initially considered the available 1-D NOE data for the *ground state* assembly under folded (or partially folded) conditions ( $T = 263$  K; CD<sub>2</sub>Cl<sub>2</sub> as solvent).<sup>2</sup> Briefly, these experiments showed that cross-coupling between nitrobenzene protons a (or b) and bipyridine protons c, d, and e is significant,<sup>5</sup> and that substantial deshielding of pyridine proton f accompanies the folding event. On this basis, a nitrobenzene face to bipyridine edge conformation is implicated. Edge-to-face ("T type") interactions are fairly common recognition elements in synthetic host-guest assemblies involving aromatic functionalities.<sup>6</sup> One subset of assemblies that has been particularly extensively studied with regard to solvent effects is Diederich's family of amine-linked cyclophane hosts with mono- and polycyclic arene guests.<sup>6</sup> For these assemblies, association is enthalpically favored and entropically disfavored, with solvent influencing the association enthalpy primarily via modulation of medium cohesive effects. This behavior has been interpreted mechanistically in terms of energy gained via solvent *self*-association when solvent molecules are displaced from the interior of the host and/or the surface of the guest.<sup>6</sup> (Conversely, energy lost in dissociating solvent molecules from either the guest or the host appears *not* to be a dominant factor in the modulation of the association strength by the medium.<sup>6</sup>) The solvent self-association effect is manifest experimentally in strong correlations of association enthalpies and free energies with empirical solvent parameters, such as Reichardt's ET(30) parameter,<sup>7</sup> which appear to measure both polarity and cohesive energy.

Attempts here to correlate  $\Delta H^\circ_{\text{folding}}$  or  $\Delta S^\circ_{\text{folding}}$  with the Reichardt scale<sup>7</sup> were unsuccessful, as were attempts with various other empirical solvent scales. On the other hand, a reasonable correlation was found between the transition temperature and the ET(30) parameter ( $r = 0.93$ ; see Figure 3)—provided that  $T_{\text{tr}}$  for methyl benzoate was (arbitrarily) excluded. (With methyl benzoate,  $r$  decreases to 0.31. The

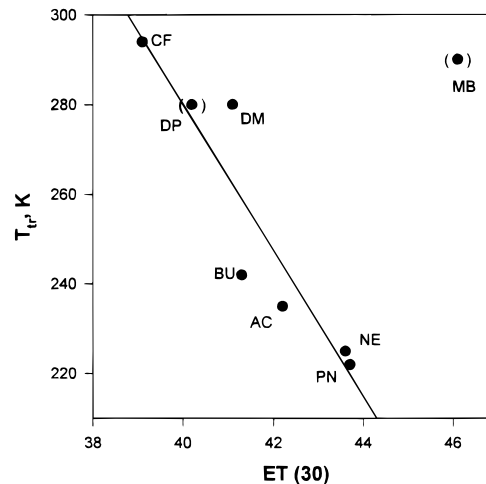


**Figure 3.** Transition temperature for excited state folding versus the ET(30) solvent parameter. Points shown in parentheses are experimentally less well defined than other points.<sup>4</sup> The line shown is a best fit line, but with arbitrary exclusion of the point for methyl benzoate. Key to solvents: NE = nitroethane, PN = propionitrile, AC = acetone, BU = butanone, DM = dichloromethane, MB = methyl benzoate, DP = dichloropropane, CF = chloroform.

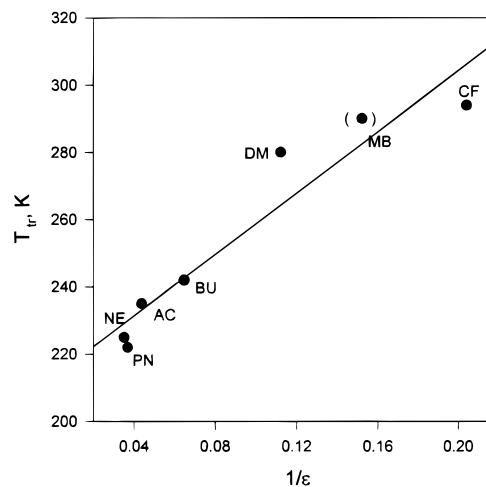


**Figure 4.** Transition temperature for excited state folding versus the inverse of the solvent dielectric constant. The point shown in parentheses is experimentally less well defined than other points.<sup>4</sup> The line shown is a best fit line through all points. See Figure 3 for key to solvents.

previously unreported value of ET(30) for methyl benzoate was measured at Northwestern by using Reichardt's dye, after reproducing published values for other solvents.)

A somewhat more compelling correlation was obtained for  $T_{\text{tr}}$  and the inverse of the solvent dielectric constant ( $r = 0.95$ ; see Figure 4). (Dichloropropane was omitted from Figure 4 because an experimental value for the dielectric constant has evidently not been reported.) Surprisingly, the correlation does not extend to  $\Delta H^\circ_{\text{folding}}$  or  $\Delta S^\circ_{\text{folding}}$ .<sup>8</sup> Conceivably these

- (4) Six of the eight solvents yield plots that clearly display two activation regimes and a well-defined transition temperature (cf. Figure 1). Methyl benzoate and dichloropropane, however, yield plots that are nonlinear, but less obviously dual component—at least over the accessible temperature ranges. Nevertheless, for completeness, we have assumed that the observed curved Arrhenius plots are dual-component plots and have reported best fit parameters (Table 1). Clearly, however, the parameters should be regarded as much less certain than those reported for other solvents.
- (5) Cross-coupling to protons g apparently also occurs, but phase-matching problems prevented us from establishing the interaction with certainty.
- (6) (a) Smithrud, D. B.; Sanford, I. C.; Ferguson, S. B.; Carcanague, D. R.; Evanseck, J. D.; Houk, K. N.; Diederich, F. *Pure Appl. Chem.* **1990**, *62*, 2227. (b) Diederich, F.; Smithrud, D. B.; Sanford, E. M.; Wyman, T. B.; Ferguson, S. B.; Carcanague, D. R.; Chao, I.; Houk, K. N. *Acta Chem. Scand.* **1992**, *46*, 205. (c) Smithrud, D. B.; Wyman, T. B.; Diederich, F. *J. Am. Chem. Soc.* **1991**, *113*, 5420.
- (7) Reichardt, C. *Solvents and Solvent Effects in Organic Chemistry*, 2nd ed.; VCH: Weinheim, Germany, 1988.

parameters, when estimated via eqs 2 and 3, could contain kinetic components in addition to the desired thermodynamic components. Regardless of the behavior of  $\Delta H^\circ_{\text{folding}}$  and  $\Delta S^\circ_{\text{folding}}$ , the transition temperature correlation in Figure 4 clearly implies that folding is enhanced in solvents of diminished dielectric strength. This, in turn, implies that the driving force for folding is predominantly Coulombic. The hydrogens of bipyridine should carry a slight positive charge which will be significantly enhanced by coordination to the dicationic rhenium center. (Recall that pyridine, rather than bipyridine, is the chromophoric ligand for the lowest MLCT transition.<sup>9</sup>) For the acceptor fragment (neutral overall), excess negative charge should be located primarily on the ketone oxygens and in the interior of the nitrobenzene ring. Coulombic association based on these distributions would be broadly consistent with the T-type geometry inferred from ground state NMR measurements.

Finally, we also examined the thermodynamics of folding in the electronic ground state. The method used was variable-temperature <sup>1</sup>H NMR, where advantage was taken of the deshielding of proton f that accompanies the folding process. An approximately 0.045 ppm shift (upfield) accompanies a temperature change from 305 to 220 K in CD<sub>2</sub>Cl<sub>2</sub> as solvent. (Below 220 K (completely folded) or above 305 K (completely unfolded) the resonance is unresponsive or only weakly responsive to changes in *T*.) The observation of intermediate shifts (single f proton resonance) at intermediate temperatures indicates that conversion between folded and unfolded forms is fast on the NMR time scale. From the relative magnitudes of the shifts, ratios of conformational populations (and, therefore, ground state folding equilibrium constants) were obtained. In addition, from the temperature dependence of  $K_{\text{folding}}$  (Figure 5) the following were obtained:  $\Delta H^\circ_{\text{folding}}(\text{ground state}) = -49 \text{ kJ mol}^{-1}$ ,  $\Delta S^\circ_{\text{folding}}(\text{ground state}) = -190 \text{ J deg}^{-1} \text{ mol}^{-1}$ , and  $T_{\text{tr}}(\text{ground state}) = 258 \text{ K}$ . The decrease in  $T_{\text{tr}}$  for ground state vs excited state folding can be rationalized on the basis of the Coulombic effects discussed above. The nominally neutral bipyridine ligand acquires a partial positive charge in the excited state as a consequence of coordination to Re<sup>II</sup>. In the ground state, however, where bipyridine is coordinated to Re<sup>I</sup>, the effective ligand charge should decrease, the strength of interaction with the partially negatively charged portion of nitrobenzene should diminish, and  $T_{\text{tr}}$  should diminish. The explanation, if

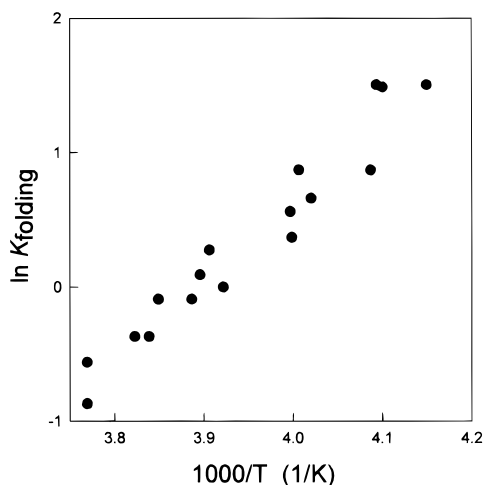


**Figure 5.** Logarithm of  $K_{\text{folding}}$  (NMR measurements; see text) versus inverse temperature in dichloromethane-*d*<sub>2</sub> as solvent.

it is fully correct, also suggests that  $-\Delta H^\circ_{\text{folding}}$  should decrease for the ground electronic state in comparison to the excited state; instead it increases. We have no explanation for the discrepancy. We note, however, that  $\Delta H^\circ_{\text{folding}}$  also varied in an apparently unpredictable fashion in the investigation of solvent effects (Table 2).

An alternative explanation for the difference between  $T_{\text{tr}}(\text{ground state})$  and  $T_{\text{tr}}(\text{excited state})$  centers on ion-pairing interactions. At the millimolar concentration levels used in the NMR experiments,  $\text{I}^+ \cdot \text{PF}_6^-$  association is probably significant. On the other hand, at the ca. 10  $\mu\text{M}$  concentration level used in the luminescence experiment, association should be largely absent. (We note, for example, that  $K(\text{association})$  is 9000  $\text{M}^{-1}$  for the ferrocene monocation and  $\text{PF}_6^-$ —an ion pair comparable in size to the assembly examined here.<sup>10</sup>) If ionic association inhibits intramolecular folding, then the observed difference in transition temperature might reflect concentration differences in the two experiments, rather than genuine ground-state/excited-state differences.

To summarize, intramolecular folding, which precedes electron transfer in **1**, is enhanced at low temperatures, enhanced in solvents of low dielectric strength, and enhanced in the metal-to-ligand charge transfer excited state in comparison to the ground state. The observations are consistent with a folding reaction that is enthalpically driven by Coulombic attraction between Re<sup>II</sup> (or Re<sup>I</sup>) coordinated bipyridine and negatively charged portions of the ester-functionalized nitrobenzene. With some data selection (perhaps justified; see above) the observations also are broadly consistent with a folding reaction that is instead driven by optimization of solvent cohesive interactions.

**Acknowledgment.** We thank the National Science Foundation (grant No. CHE-9303682, predoctoral fellowship for R.V.S., and traineeship for A.P.K.) for support of our work. J.T.H. also acknowledges support from the Camille and Henry Dreyfus Foundation (Teacher-Scholar Award, 1991–6).

**Supporting Information Available:** A figure showing an apparent correlation between enthalpic and entropic folding parameters (1 page). Ordering information is given on any current masthead page.

IC950534E

- (8) Curiously, however, these parameters correlate extremely well with each other ( $r = 0.97$ ; see Supporting Information) and with various kinetic parameters. While it is tempting to attach detailed chemical significance to the correlations, other explanations may exist. The  $\Delta H^\circ_{\text{folding}}/\Delta S^\circ_{\text{folding}}$  correlation, for example, might signify only that the range of transition temperatures for the available solvents is relatively small. (Note that a statistically perfect correlation between solvent-dependent enthalpies and entropies would necessarily exist if  $T_{\text{tr}}$  were the same for all solvents.) Krug et al. (*Nature* **1976**, 261, 566; *J. Phys. Chem.* **1976**, 80, 2235, 2341) have pointed out that apparent enthalpy/entropy correlations can readily arise from a correlated propagation of experimental errors. They argue that free energy vs enthalpy correlations, at an average experimental temperature, offer a means for assessing the chemical validity of enthalpy/entropy correlations (since experimental errors for the former should be statistically uncorrelated). The data in Table 2 fail this test ( $r = 0.28$ ), indicating that the correlations are likely spurious.
- (9) A reviewer has pointed out that if the Coulombic explanation is correct, the excited-state folding equilibrium could likely be altered by derivatizing the bipyridyl ligand so as to yield a ligand-localized  $\pi-\pi^*$  state, in place of the charge transfer state, as the lowest-lying excited state.

- (10) Blackburn, R. L.; Hupp, J. T. *J. Phys. Chem.* **1993**, 97, 3278.